A novel real-time measurement method for dynamic resistance signal in medium-frequency DC resistance spot welding

Ze-Wei Su[1], Yu-Jun Xia[1], Yan Shen[1] and Yong-Bing Li[1,2,3]

[1] Shanghai Key Laboratory of Digital Manufacture for Thin-walled Structures, School of Mechanical Engineering, Shanghai Jiao Tong University, Shanghai 200240, People's Republic of China
[2] State Key Laboratory of Mechanical System and Vibration, Shanghai Jiao Tong University, Shanghai 200240, People's Republic of China

E-mail: yongbinglee@sjtu.edu.cn

Abstract

Resistance spot welding (RSW) is widely used in auto-body manufacturing, and the weld quality is critical to ensure the safety and reliability of an automobile structure. The dynamic resistance (DR) signal is one of the most frequently applied process signals for real-time quality monitoring and control of RSW. However, the accuracy of DR measurement is highly affected by the inductive component of the secondary voltage signal. In a medium-frequency direct-current (MFDC) RSW system, it is proven that traditional DR measurement methods such as the root mean square (RMS) method and average method fail to eliminate the interference of inductance, and barely meet the monitoring requirements. Therefore, a novel real-time DR measurement method based on a forgetting-factor recursive least square algorithm is proposed and tested under simulated and experimental conditions in this paper. Sensitivity analysis is performed to optimize the forgetting factor, which is proven to be the critical parameter of the novel method to balance the convergence speed and oscillation amplitude. With the optimized forgetting factor, the error analysis and comparative study are conducted under different welding modes. The results show that the inductive noise can be effectively eliminated by the new method. The measurement error of the proposed method is limited within $\pm 6 \ \mu\Omega$ at a 99.73% confidence level ($\pm 3\sigma$) at both constant and time-varying current modes. This study can pave the way for real-time monitoring and control for an MFDC RSW system.

Keywords: resistance spot welding, medium-frequency direct current, dynamic resistance, real-time measurement, forgetting factor

(Some figures may appear in colour only in the online journal)

1. Introduction

Resistance spot welding (RSW) is the major joining method for car-body manufacturing [1], and the weld quality directly affects the auto-body security and reliability. The quality of RSW is significantly influenced by various disturbances in the production sites [2], which makes the welding quality inspection critical. Traditional direct RSW quality inspection methods, such as sampling inspection based on destructive or non-destructive techniques, are inefficient and cannot inspect 100% of the welds on a car body. As a result, reliable non-destructive techniques of RSW quality monitoring by measuring various dynamic signals are generally proposed, such as dynamic resistance (DR) [3–11], electrode force [12–14], electrode vibration signals [15], ultrasonic signal [16–18] and electrode displacement [19–23], to reflect the nugget

[3] Author to whom any correspondence should be addressed.
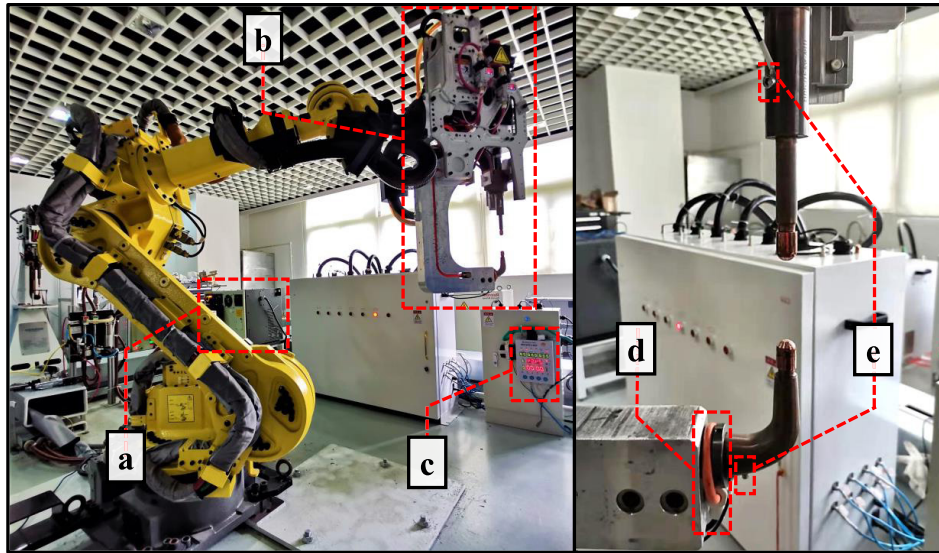
Figure 1. Experimental equipment and measuring sensors. (a) Welding controller, (b) spot-welding robot, (c) signal-processing equipment, (d) Rogowski coil, (e) wire for voltage measurement.

growth process indirectly. DR monitoring is widely accepted because it is low-cost and can provide rich information on nugget formation [24–26]. Since metal melting and solidifying processes occur at the interfaces of steel sheets that are not visible, it is challenging to observe nuggets and get the true value of DR accurately in real time. Hence, researchers have conducted many in-depth studies on DR measurement methods.

Several DR measurement methods have been applied to AC RSW equipment. Andrews *et al* [3] measured the DR of one cycle or half-cycle with the ratio of the RMS voltage to RMS current. Savage *et al* [4] calculated DR by using the instantaneous electrode voltage and welding current at the peak current point in each half-cycle to remove the inductive noise caused by the transformer. Needham *et al* [27] calculated DR by the ratio of integrated voltage and integrated current to theoretically eliminate the induced noise. Yongjoon Cho *et al* [5] used the process variables, which were monitored in the primary circuit of the welding machine, to obtain the variation in DR across electrodes. Garza and Das *et al* [6, 7] used a recursive least square (RLS) method to iteratively calculate the resistance and inductance, which improved the sampling resolution of the signal. Ling and Wong *et al* [8, 9] used the Hilbert transform to monitor the time-varying input impedance signal. Hongjie Zhang and Lijing Wang *et al* [10, 11] proposed a new measurement method to obtain the complex electrical impedance, the real part of which reflects the DR changes, and provided more details over time.

In recent years, the technology of the mid-frequency DC (MFDC) inverter has become more mature. The secondary current of an MFDC RSW has no zero-crossing phenomenon of the welding current, which provides a good condition for realizing DR monitoring technology [28, 29]. The peak value method [4] cannot be used in MFDC RSW, because its secondary current signal does not have a peak with a derivative of zero. The root mean square (RMS) method [3] and the

average method [27] are the most widely used methods to monitor the DR used in MFDC RSW controllers. When measuring the voltage, the impedance of the RSW circuit consists of two parts: the resistance load containing the DR relating to weld nugget formation, and the inductive reactance caused by the mutual inductance and internal inductance of the circuit [30]. As a result, DR cannot be measured by merely dividing the voltage by the current. The measurement accuracies of the traditional methods are highly affected by the inductive component of the secondary voltage and barely meet the monitoring requirements.

In this study, a novel real-time measurement method for the DR signal in MFDC RSW is presented, which can eliminate inductive noise and measure the resistance accurately. Therefore, a measuring system was built to measure the current and voltage signals of MFDC RSW. Sensitivity analysis was conducted to determine the optimal value of the method key parameter through simulation experiments. In addition, a series of welding experiments under different welding modes were carried out, and error analysis and comparative study were conducted to test the accuracy of the new method in measuring the DR of MFDC RSW.

2. DR measurement system and the equivalent circuit

Real-time electrical welding signals were required to measure the DR during the RSW process. The whole experimental system consisted of several parts as shown in figure 1, including a welding controller, spot welding robot, signal processing equipment and measurement sensors for current and voltage. A Centerline spot-welding robot with a servo gun was used, and the resistance welding controller was an MEDAR(WTC) MFDC adaptive controller with a working frequency of 1000 Hz. The electrodes used in the
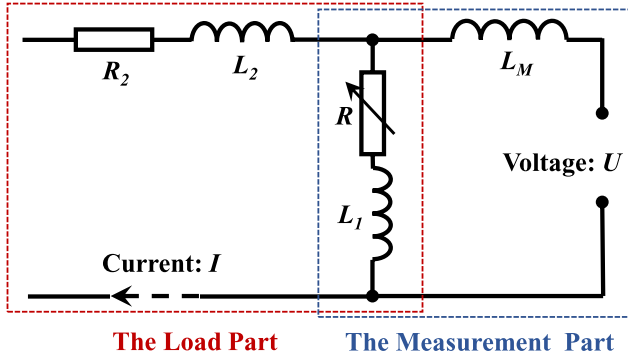
Figure 2. Equivalent circuit of MFDC RSW.

experiments were made of a CuCrZr alloy with an end face of 6 mm in diameter. In this study, a MEATROL Rogowski coil of 0.5% accuracy class was placed on the lower electrode as the current sensor. Its output signal could be used to obtain the current signal through integration by the signal-processing equipment. The integral constant of the integrator was 20 ms and the sampling frequency was 240 ksps, which means it could obtain 240 000 samples per second. This Rogowski coil exhibited a strong anti-interference ability and high measurement accuracy, meeting the measurement requirements of the MFDC RSW secondary current. Two shielded twisted pairs were installed on the mounting holes on the upper and lower electrode arms to record the secondary voltage.

A typical equivalent circuit for the load part and the measurement part of the secondary circuit of MFDC RSW is shown in figure 2, which is equivalent to a resistor–inductor series (RL) circuit model [31–33]. In the figure, L_1 and L_2 represent the inductance of the RSW secondary circuit (L_1 is the inductance within the measurement area and L_2 is the inductance outside the measurement area); L_M is the mutual inductance generated during the voltage measurement under a time-varying electromagnetic field; R is the resistance in the measurement area and changes continuously as the nugget is formed, which usually consists of the contact resistance, the electrode resistance of the electrode and the sheets; and R_2 is the total resistance outside the measurement area. During the RSW process, the welding transformer is used to induce a voltage as the input source in the secondary circuit. Two or more metal sheets are pressed together by a pair of electrodes, and the passage of large current heats up the sheets through the resistance in accordance with Joule's Law. The voltage U measured by the twisted-pair cablings in the RSW process can be expressed as equation (1), which is available from the equivalent circuit model and composed of a resistive and an inductive component [30]:

$$U = IR + L\frac{\mathrm{d}I}{\mathrm{d}t}. \tag{1}$$

In the equation, I is the secondary current and L is the total inductance of L_1 and M. R is the resistance load. Due to the total inductance L, DR cannot be calculated by merely dividing the voltage by the current.

3. Novel real-time measurement method for DR signal

3.1. Algorithm for calculating DR

The RLS method, characterized by stronger tracking ability and fast calculation speed, has been widely used as an adaptive parameter identification method [34–36]. It is less sensitive to noise and can be measured according to the process. The difference between the actual observed and calculated values of information can be minimized to estimate the unknown parameters of the model. Thus, this method is widely used in the field of online parameter identification. Based on the equivalent RL circuit model of the secondary circuit and equation (1), the voltage of the secondary circuit is expressed as equation (2):

$$u = h\theta \quad h = \begin{pmatrix} I & \frac{\mathrm{d}I}{\mathrm{d}t} \end{pmatrix}, \quad \theta = \begin{pmatrix} R \\ L \end{pmatrix}. \tag{2}$$

According to equation (2), the discernibility matrix θ consists of the resistance R and the inductance L. h is the regression matrix constructed from the current I and current differential composition $\mathrm{d}I/\mathrm{d}t$. However, a so-called 'data saturation' phenomenon occurs in the RLS method as the data grow, which means that the information provided by the new data is drowned out by the old data and gradually loses effect on the correction of parameter estimates [37–39]. The gain matrix used to correct the previous discernibility matrix also gradually decreases until it approaches 0, which means the algorithm can no longer effectively correct the parameter. In order to mitigate this phenomenon, the attenuation factor β $(0 < \beta < 1)$ is added to reduce the impact of the old data by exponentially weighting it, and increase the impact of the new data to adapt to the rapid change of time-varying signals. The model at the kth sampling point can be described by equation (3):

$$\begin{pmatrix} \beta^{k-1}u(1) \\ \vdots \\ \beta^{k-k}u(k) \end{pmatrix} = \begin{pmatrix} \beta^{k-1}h^T(1) \\ \vdots \\ \beta^{k-k}h^T(k) \end{pmatrix} \theta(k) \tag{3}$$

$$\theta(k) = \left[\begin{pmatrix} \beta^{k-1}h^T(1) \\ \vdots \\ \beta^{k-k}h^T(k) \end{pmatrix}^T \begin{pmatrix} \beta^{k-1}h^T(1) \\ \vdots \\ \beta^{k-k}h^T(k) \end{pmatrix} \right]^{-1}$$
$$\left[\begin{pmatrix} \beta^{k-1}h^T(1) \\ \vdots \\ \beta^{k-k}h^T(k) \end{pmatrix}^T \begin{pmatrix} \beta^{k-1}u(1) \\ \vdots \\ \beta^{k-k}u(k) \end{pmatrix} \right]. \tag{4}$$

Based on the modified circuit equation (3), the calculation formula (4) of the identification matrix $\theta(k)$, which represents the resistance and inductance of the kth sampling point, can be obtained. The resistance R and inductance L of the secondary circuit are estimated based on the current I and voltage u provided during welding. Then, the covariance matrix $P(k)$ is defined as equation (5), which demonstrates the relationship

between $P(k)$ and $P(k-1)$ to service for subsequent iterations, where $\alpha = \beta^2$ is defined as the forgetting factor:

$$P(k) = \left[\begin{pmatrix} \beta^{k-1}h^T(1) \\ \vdots \\ \beta h^T(k-1) \\ h^T(k) \end{pmatrix}^T \begin{pmatrix} \beta^{k-1}h^T(1) \\ \vdots \\ \beta h^T(k-1) \\ h^T(k) \end{pmatrix} \right]^{-1}$$

$$= \left[\beta^2 \left(\begin{pmatrix} \beta^{k-2}h^T(1) \\ \vdots \\ \beta h^T(k-2) \\ h^T(k-1) \end{pmatrix}^T \begin{pmatrix} \beta^{k-2}h^T(1) \\ \vdots \\ \beta h^T(k-2) \\ h^T(k-1) \end{pmatrix} \right) + h(k)h^T(k) \right]^{-1}$$

$$= \left[\alpha P^{-1}(k-1) + h(k)h^T(k) \right]^{-1}$$

$$= \frac{1}{\alpha} \left[I - \frac{P(k-1)h(k)h^T(k)}{h^T(k)P(k-1)h(k) + \alpha} \right] P(k-1). \tag{5}$$

The discernibility matrix is transformed into equation (6) with the covariance matrix $P(k)$ and shows the relationship between $\theta(k)$ and the matrix on the previous point $\theta(k-1)$. The previous discernibility matrix is used to obtain the new one by correcting the error between the observed matrix $u(k)$ and the predicted value $h^T\theta(k-1)$:

$$\theta(k) = P(k) \begin{pmatrix} \beta^{k-1}h^T(1) \\ \vdots \\ \beta h^T(k-1) \\ h^T(k) \end{pmatrix}^T \begin{pmatrix} \beta^{k-1}u(1) \\ \vdots \\ \beta^{k-k}u(k) \end{pmatrix}$$

$$= P(k) \left[\alpha P^{-1}(k-1)\theta(k-1) + h(k)u(k) \right]$$

$$= \left[I - P(k)h(k)h^T(k) \right] \theta(k-1) + P(k)h(k)u(k)$$

$$= \theta(k-1) + P(k)h(k) \left[u(k) - h^T(k)\theta(k-1) \right]. \tag{6}$$

$K(k)$, which is called the gain matrix and indicates the degree of correction for errors, is calculated by equation (7). The larger the gain matrix $K(k)$, the stronger the correction effect:

$$K(k) = P(k)h(k)$$

$$= \frac{1}{\alpha} \left[I - \frac{P(k-1)h(k)h^T(k)}{h^T(k)P(k-1)h(k) + \alpha} \right] P(k-1)h(k)$$

$$= \frac{P(k-1)h(k)}{h^T(k)P(k-1)h(k) + \alpha}. \tag{7}$$

Finally, the forgetting-factor recursive least square (FFRLS) algorithm used to decouple the resistance and inductance values of the kth sampling point is summarized as the above equations where $0 \leqslant \alpha \leqslant 1$:

$$\begin{cases} \theta(k) = \theta(k-1) + K(k) \left[u(k) - h^T(k)\theta(k-1) \right] \\ K(k) = \dfrac{P(k-1)h(k)}{h^T(k)P(k-1)h(k) + \alpha} \\ P(k) = \dfrac{1}{\alpha} \left[I - K(k)h^T(k) \right] P(k-1). \end{cases} \tag{8}$$

The FFRLS method for resistance measurement was proposed with the algorithm. The flow chart of the new method is shown in figure 3, where M is the total number of sampling points and T is the cycle time corresponding to the carrier frequency. The regression matrix $h(k)$ is built from the secondary current I and the relevant current differential $\mathrm{d}I/\mathrm{d}t$. The
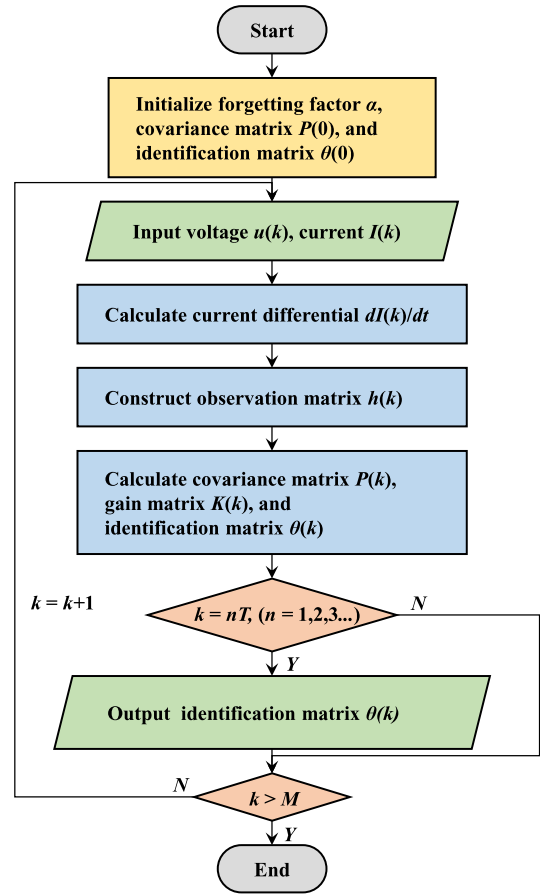

Figure 3. Flow chart of the FFRLS method.

voltage value at the kth sampling point in the welding process needs to be collected as the observation matrix $u(k)$. During the measurement process, the forgetting factor α was used to prevent the information being incorporated into the old data. The regression matrix $h(k)$ is initialized as zero, while the gain matrix $K(k)$ and the covariance matrix $P(k)$ are both initialized as the identity matrix. Based on the error between the observation matrix $u(k)$ and the result value calculated by the regression matrix $h(k)$, the gain matrix $K(k)$ and the covariance matrix $P(k)$ are calculated. Then, the discernibility matrix $\theta(k)$ is obtained by correcting the previous discernibility matrix. As the new observation data are introduced periodically, the FFRLS method decouples the inductance and resistance at every sampling point through iteration, and then outputs the discernibility matrix per cycle time T. Through continuous iterative correction within a cycle, the estimated values of DR and inductance within a cycle are obtained. As shown in each subfigure of figures 9 and 12, the FFRLS method can measure resistance accurately in MFDC RSW and meet the monitoring requirements.

3.2. Determination of optimal forgetting factor by sensitivity analysis

The forgetting factor α used in the FFRLS method is the key to avoiding incorporation of the new data into the old data. If the forgetting factor decreases, the tracking ability of the system
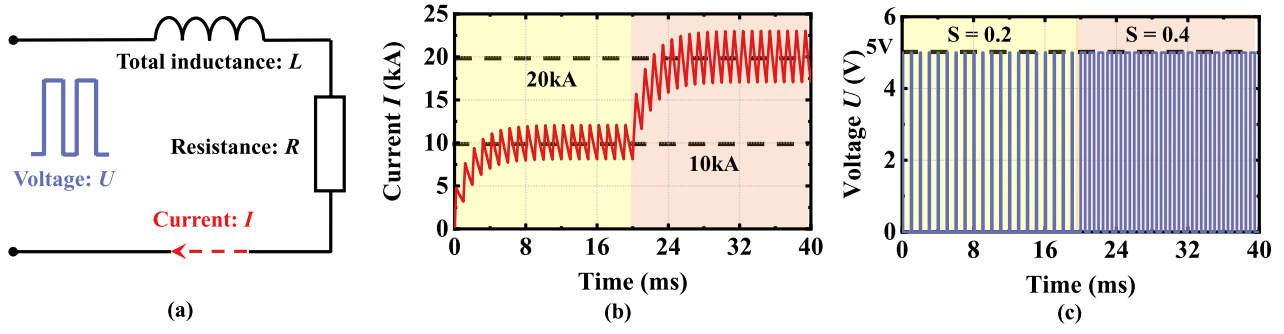
Figure 4. Simulation results of secondary signal when welding with the time-varying current. (a) Secondary circuit model, (b) secondary current, (c) secondary voltage. *S* is the duty cycle.
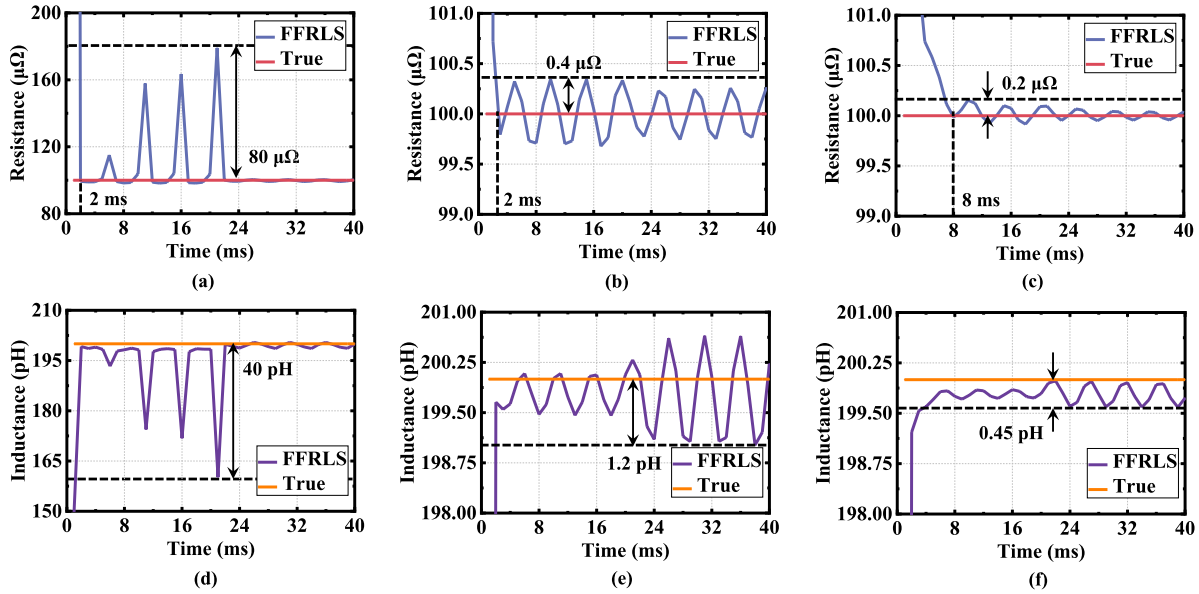

Figure 5. Resistance and inductance measured at different forgetting factors. (a) Resistance at forgetting factor 0.95, (b) resistance at forgetting factor 0.98, (c) resistance at forgetting factor 0.99, (d) inductance at forgetting factor 0.95, (e) inductance at forgetting factor 0.98, (f) inductance at forgetting factor 0.99.

will become stronger to track the variation of resistance in time but it will also be more sensitive to noise. If the value of the forgetting factor becomes larger, the oscillation amplitude will decrease, but the tracking ability of the system will be weakened. Therefore, the optimal forgetting factor needs to be determined by sensitivity analysis so that the tracking ability is guaranteed and noise interference is reduced. A series of simulated welding experiments were carried out for sensitivity analysis and to test the algorithm's ability to decouple resistance and inductance. Since the changes of the transformer leakage inductance and the transformation ratio can be equivalent to a change in the input voltage waveform, they can be ignored in the simulation because they have less effect on the algorithm verification and forgetting factor optimization. The simulation was conducted using circuit balance equations where the inversion period is set as T, the duty cycle is S, the peak value of the secondary voltage is U_M, the initial moment is t_0, the current is i, the DR is R and the inductance is L. Based on the set values, the currents are obtained by circuit balance equations. When $(n-1)T \leqslant t_0 + t \leqslant (n-1)T + TS$, the magnitude of the obtained current is

$$\mathrm{i}(t_0 + t) = \frac{U_M}{R} + \left[\mathrm{i}(t_0) - \frac{U_M}{R}\right] \cdot \mathrm{e}^{-\frac{R}{L}t}. \tag{9}$$

When $(n-1)T + TS \leqslant t_0 + t \leqslant (n)T$, the magnitude of the obtained current is

$$\mathrm{i}(t_0 + t) = \mathrm{i}(t_0) \cdot \mathrm{e}^{-\frac{R}{L}t}. \tag{10}$$

The obtained current signal (after applying noise) and the set voltage signal can be used to simulate the welding experiment to select an optimal forgetting factor and to test the algorithm's ability to decouple resistance and inductance. In the simulation experiments, the secondary voltage peak was 5 V, the welding time was 40 ms, the resistance was 100 μΩ, and the total inductance L that is made up of the circuit inductance in the measurement area L_1 and the mutual inductance L_M was 0.2 pH. The inversion period was set as 1 ms and 240 points were sampled in one period. A step current signal from about 10 kA to 20 kA was generated to the simulated welding with the duty cycle of the voltage changed from 20% to 40% at 20 ms in the experiments, as shown in figure 4. Simulated sinusoidal noise of ±20 A was applied to the current during resistance measurement.
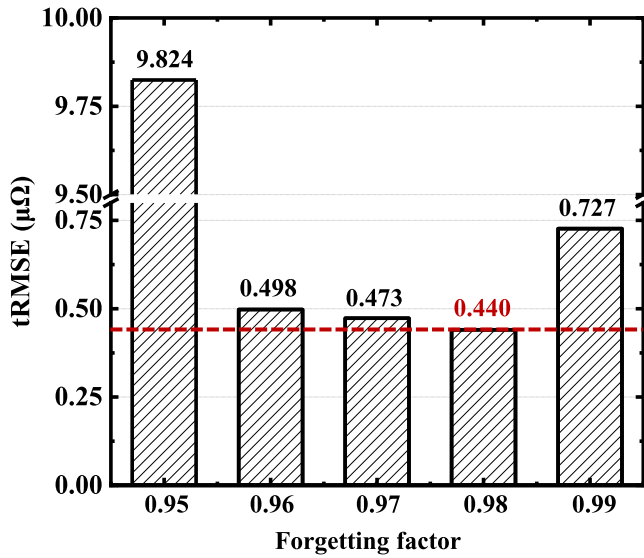
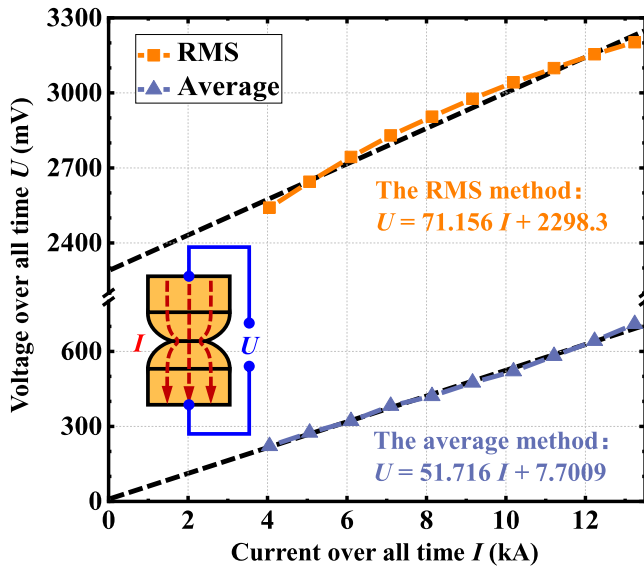**Figure 6.** tRMSE of DR curves with different forgetting factors.

Figure 7. Volt–ampere characteristic curves measured by the RMS method and the average method.

The different forgetting factors were tested and analyzed in this study, as shown in figure 5. When the forgetting factor is smaller than 0.98, the FFRLS method can track the resistance variation in time, but it is particularly sensitive to noise. When the forgetting factor is 0.95, the maximum error caused by noise can even reach 80 μΩ. If the forgetting factor exceeds 0.98, the DR curve becomes smoother with the increase in the forgetting factor, and the tracking ability is weakened. An 8 ms delay even occurs at the beginning of welding with forgetting factor 0.99. In addition, the FFRLS method can also accurately measure the inductance component. The error of inductance continues to decrease as the forgetting factor continues to increase. When the forgetting factor is 0.98, the maximum error of resistance measurement is about 0.4 μΩ with a 2 ms delay, and the maximum error of inductance measurement is 1.2 pH.
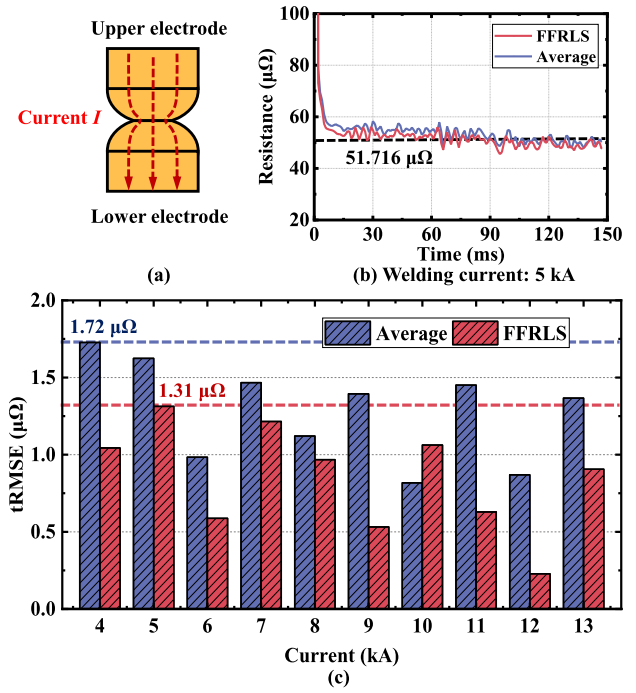

Figure 8. Results when welding with no sheets and constant currents. (a) Schematic diagram for the RSW process, (b) resistance when welding current is 6 kA, (c) tRMSE of the FFRLS method and the average method.

Table 1. Chemical composition of applied steel sheet (mass %).

Steel grades	C	Si	Mn	P	S	Alt
DP590	0.055	0.507	1.616	0.010	0.004	0.048

In resistance measurements, the error of the method defined as the tRMSE is calculated by equation (11) to evaluate the accuracy of the new methods, where M is the total number of sampling points in a DR curve and $e(i)$ is the error between the measured value and the true value at the ith sampling point:

$$tRSME = \sqrt{\frac{1}{M}\sum_{i=1}^{M} e(i)^2}. \tag{11}$$

The optimal forgetting factor was obtained by comparing the tRMSE with different forgetting factors. Furthermore, the tRMSE with forgetting factor from 0.95 to 0.99 is shown in figure 6. When the forgetting factor is 0.98, the value of the tRMSE reaches a minimum of 0.44 μΩ. Moreover, the high convergence rate of the new method means that this method can realize real-time tracking and accurately feed back the variation of resistance in the RSW process. The process of determining the optimal forgetting factor is actually to find the balance point between the convergence speed of the algorithm and the ability to resist noise interference. The forgetting factor is only related to the sampling parameters of the monitoring equipment, and does not need to be changed to cater to the new welding condition. From the results of simulated
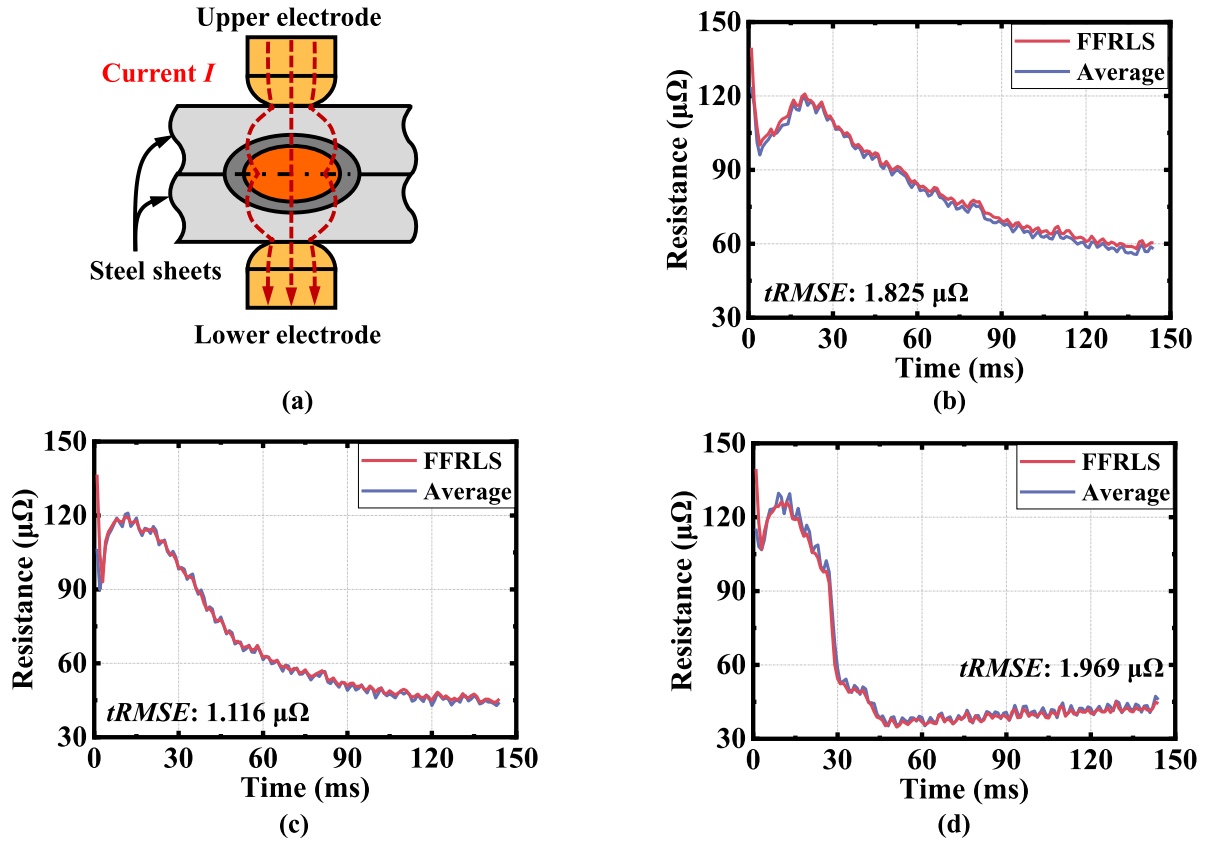
Figure 9. Resistance when welding with steel sheets and constant currents. (a) Schematic diagram for the RSW process, (b) welding current: 6 kA, (c) welding current: 9 kA, (d) welding current: 12 kA.

welding, the optimal forgetting factor 0.98 meets the actual RSW monitoring requirements with a sampling frequency of 240 ksps.

4. Error analysis for the new method

4.1. With the constant current mode

The effectiveness and reliability of the traditional DR measurement methods were tested in welding experiments. The RMS method [3] and the average method [27] measure the resistance of one cycle according to Ohm's law, and the voltage and current of one cycle should be measured first. The time of one cycle is 1 ms, and 240 data points are used for resistance recognition in one cycle. The RMS voltage of one cycle U_{rmst} and the RMS current of one cycle I_{rmst} are simultaneously calculated by equation (12), where T represents the cycle time corresponding to the carrier frequency, i represents the instantaneous current, and u represents the instantaneous voltage. The average current of one cycle $\overline{I_t}$ and the average voltage of one cycle $\overline{U_t}$ are used in equation (13) to calculate the resistance of one cycle $\overline{R_t}$:

$$R_{\mathrm{rmst}} = U_{\mathrm{rmst}}/I_{\mathrm{rmst}} \quad U_{\mathrm{rmst}} = \sqrt{\frac{1}{T}\int_T u^2 \mathrm{d}t}, I_{\mathrm{rmst}} = \sqrt{\frac{1}{T}\int_T i^2 \mathrm{d}t} \tag{12}$$

$$\overline{R_t} = \overline{U_t}/\overline{I_t} \quad \overline{U_t} = \frac{1}{T}\int_T u\mathrm{d}t, \overline{I_t} = \frac{1}{T}\int_T i\mathrm{d}t. \tag{13}$$

Although it is hard to get the true value of DR, it is obvious that the DR remains basically unchanged when welding with no sheet, and the accurate value can be obtained by the volt–ampere characteristic curve. The welding experiments were carried out with constant current and no sheet was placed between the electrodes. The secondary current was set to 4 kA and to 13 kA in turn, and the welding time was 150 ms. When welding with constant current, voltage and current remain approximately unchanged during the welding process. The volt–ampere characteristic curves of the RMS method and the average method were drawn with the values over all time such as U_{rms} and I_{rms}, the slope of which was the resistance of the measurement area, as shown in figure 7. The values over all time, such as U_{rms} and $\overline{U}$, could be calculated by the average of the value of one cycle during the whole welding process, such as U_{rmst} and $\overline{U_t}$.

The volt–ampere characteristic curve measured by the RMS method has a broad intercept (1082.3 mV), indicating that there is a sizeable error caused by inductance in the resistance measurement of the RMS method. By contrast, the intercept of the volt–ampere characteristic curve measured by the average method (7.7 mV) is approximately zero following the pure resistance load law, so the slope of the curve calculated by the average method (51.716 μΩ) is considered as the conventional true value of the measuring area resistance. Furthermore, the RMS current differential dI/dt of one cycle is never zero, so the inductive component of voltage in equation (1) always exists and is greater than 0. The resistance
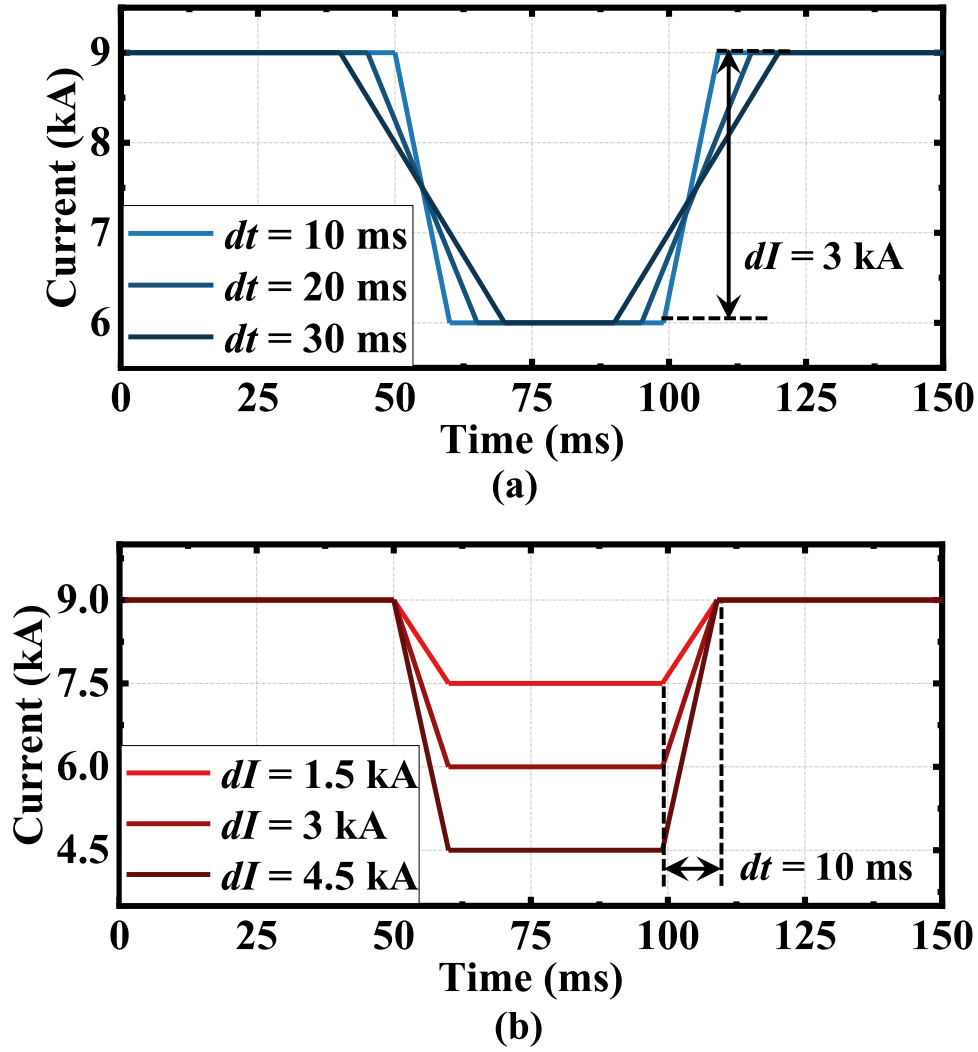
Figure 10. Time-varying current with different degrees and times of variation used in the experiments. (a) Current with times of variation d*t*, (b) current with degrees of variation d*I*.

of one cycle R_{rmst} calculated by dividing the voltage by the current simply always contains inductive noise. However, the average current differential d*I*/d*t* of one cycle changes negatively with an exponential decay to zero, and the average of the inductive components in the secondary voltage also decays negatively with time when the current is constant. As a result, the resistance of one cycle $\overline{R_t}$ measured by the average method is almost accurate.

Following the RSW theory, the temperature of the secondary circuit is low when welding with no sheet, and the resistance value of the measurement area should remain stable at the true value. The tRMSE of the FFRLS method and the average method at different currents from 4 kA to 13 kA are compared to analyze the accuracy of the new method when the current is constant, as shown in figure 8(c), where the true value is replaced by the conventional true value. Only the data of 10–150 ms is employed for the tRMSE calculation. The maximum tRMSE of the FFRLS method compared to the conventional true value is 1.31 μΩ, less than the maximum value of the average method 1.72 μΩ. As an example, the DR curves of the FFRLS method and the average method are almost stable at the conventional true value of the measuring area

resistance 51.716 μΩ when welding with the constant current 5 kA, as shown in figure 8(b). The results show that the new method and the average method can both eliminate the inductive noise to measure the resistance of one cycle. As a result, when welding with the constant current mode, the measurement accuracy of the new method and the average method are both better than that of the RMS method.

From the error analysis theory, the population standard deviation and probability limit error are calculated for random error evaluation of the new method. The population standard deviation σ can be estimated by

$$\sigma = \sqrt{\frac{1}{l-1}\sum_{p=1}^{l}\left(tRMSE(p)\right)^2} \qquad (14)$$

where $tRMSE(p)$ is used to represent the random error of the pth measured series and l is the total number of measured series. Thus, the population limit error can be calculated by multiplying the confidence coefficient by the population standard deviation, where the coefficient usually takes 3 for a 99.73% confidence level ($\pm 3\sigma$). It can be calculated that the random errors are 0.958 μΩ and the probability limit error
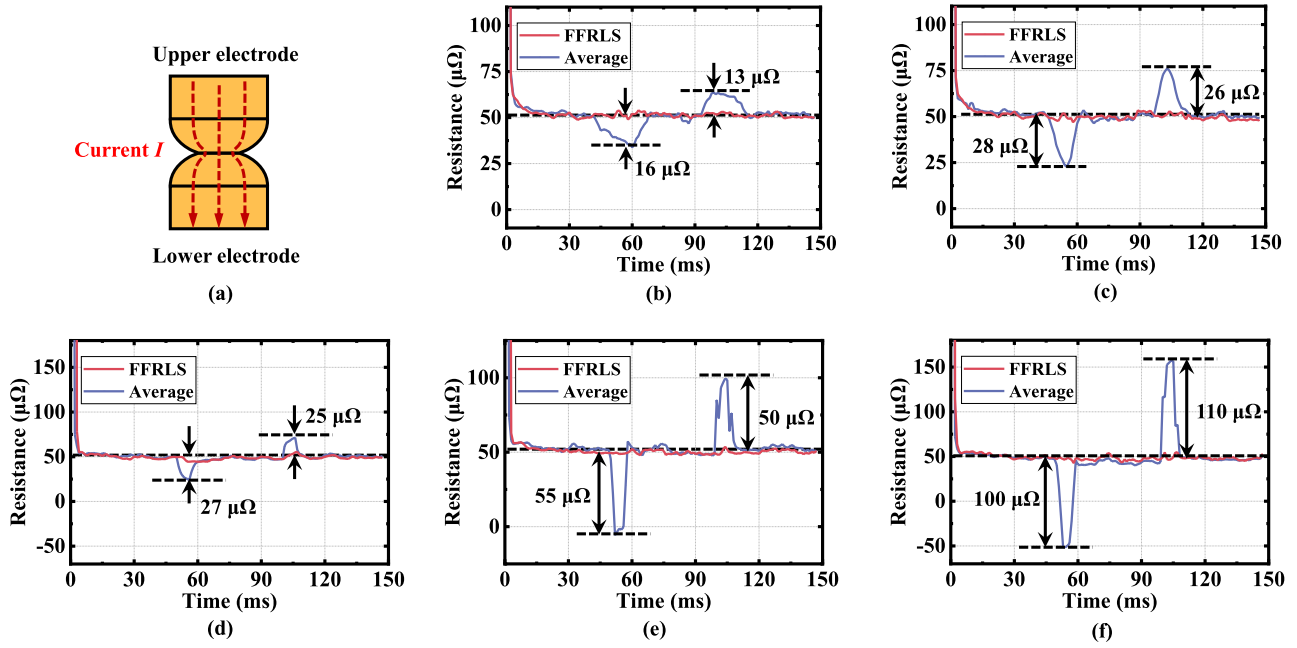
Figure 11. Resistance measured when welding with no sheet and different time-varying current modes. (a) Schematic diagram for the RSW process, (b) dI = 3 kA, dt = 30 ms, (c) dI = 3 kA, dt = 20 ms, (d) dI = 1.5 kA, dt = 10 ms, (e) dI = 3 kA, dt = 10 ms, (f) dI = 4.5 kA, dt = 10 ms.

of the DR curves measured by the FFRLS method is mainly distributed in $\pm 3 \, \mu\Omega$ when welding with the constant current mode.

Additionally, two uncoated DP590 high-strength steel sheets of 0.8 mm thickness and tensile strength of $\geqslant$590 MPa were used to test the error of the methods with a constant current. The chemical composition of the steel is given in table 1. Welding experiments under three current levels (6 kA, 9 kA, 12 kA) were performed, where the electrode force was set as 2.6 kN and the welding time as 150 ms. The tRMSE between the measured resistance value and true value is analyzed to test the method calculation precision, as shown in figure 9. Because it is difficult to get the true value in actual welding, the resistance measured by the average method is viewed as the conventional true value to calculate the tRMSE in actual welding. As shown in the results, the tRMSE is less than $2 \, \mu\Omega$, which means that the value obtained by the FFRLS method is very similar to the conventional true value and the measurement error of the proposed method is limited within $\pm 6 \, \mu\Omega$ at a 99.73% confidence level in actual welding. The DR curves measured by the FFRLS method conform to the DR change law during RSW: rapid drop, fast rise and slow decline. The features extracted from the DR curves are closely related to the welding process and offer more information for welding quality monitoring. With the increased welding current, significant differences can be seen; for example, DR variation increases and the DR peak times are advanced. The sudden drop in DR curves in figure 9(d) reflects the RSW expulsion when the current is large. The new method with a higher resistance measurement accuracy can assist in exploring the correlation between the DR features and weld quality indicators.

Table 2. tRMSE with different time-varying current modes.

Mode	Current modes		tRMSE	
	dI (kA)	dt (ms)	Average ($\mu\Omega$)	FFRLS ($\mu\Omega$)
1	3	10	14.134	1.514
2	3	20	8.321	1.826
3	3	30	6.253	1.789
4	1.5	10	6.652	1.384
5	4.5	10	28.212	1.997

4.2. With the time-varying current mode

Welding experiments with no sheet were performed to compare the measurement accuracy of the new method and the average method as the current varies, where the electrode force was set to 2.6 kN. The time-varying current was set to three-stage, and the total welding duration was 150 ms. In the welding experiments, different times of variation (10 ms, 20 ms and 30 ms) were applied to welding experiments to analyze the error introduced by the current variation as shown in figure 10(a), where the three-stage current was fixed at 9 kA—6 kA—9 kA. In addition, different degrees of current variation dI (1.5 kA, 3 kA and 4.5 kA) were set by changing the magnitude of the second stage (7.5 kA, 6 kA and 4.5 kA) as shown in figure 10(b), in which the first and third stages were set to 9 kA and the time of variation was set to 10 ms.

It is proven in this article that the resistance value of the measurement area should remain stable at the true value when welding with no sheets. Because of the immediacy and invisibility of RSW, the conventional true value 51.716 $\mu\Omega$ is taken as the true value. The DR curves obtained by the average method and the FFRLS method are both stable when the
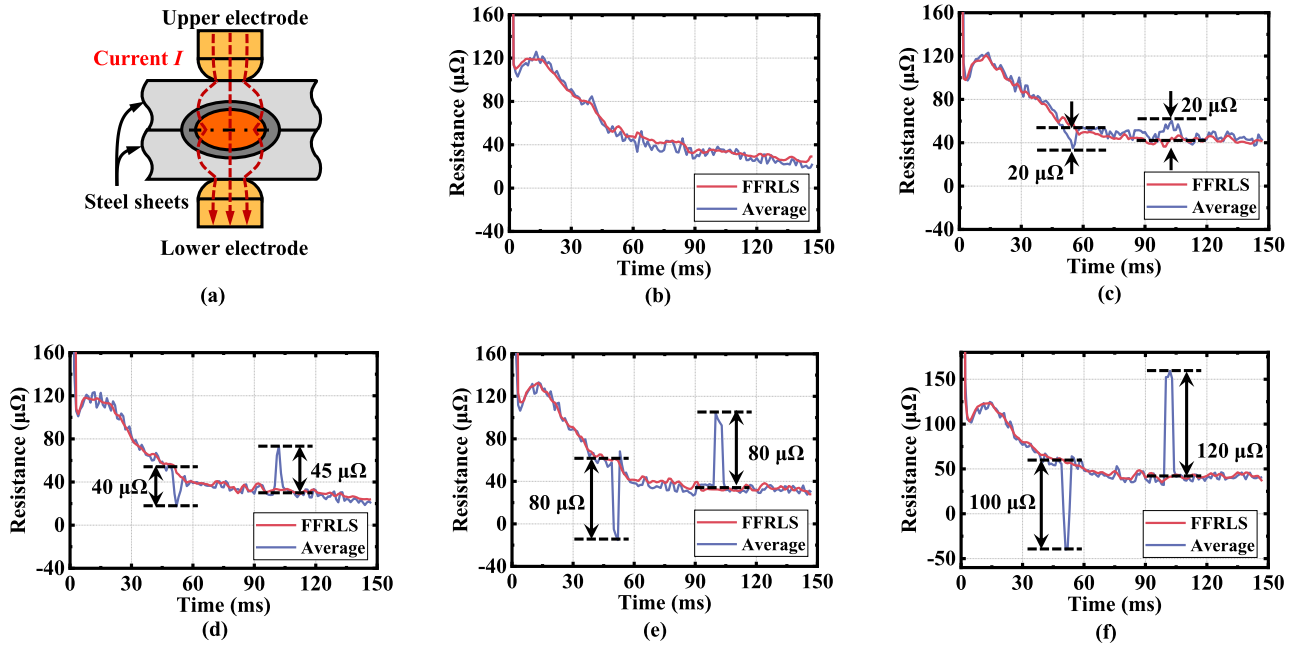
Figure 12. Resistance measured when welding with steel sheets and time-varying current. (a) Schematic diagram for the RSW process, (b) dI = 3 kA, dt = 30 ms, (c) dI = 3 kA, dt = 20 ms, (d) dI = 1.5 kA, dt = 10 ms, (e) dI = 3 kA, dt = 10 ms, (f) dI = 4.5 kA, dt = 10 ms.

current remains constant. As dt increases from 10 ms to 30 ms, the error of the average method is reduced from 55 $\mu\Omega$ to 16 $\mu\Omega$, as shown in figures 11(b), (c) and (e). It is also shown in figures 11(d)–(f) that the error of the average method reaches 27 $\mu\Omega$ as the current varies by 1.5 kA, and the error increases to about 110 $\mu\Omega$ as the degree of current variation dI increases to 4.5 kA. In general, when the current varies quickly and the value of dI/dt increases, the resistance error of the average method grows larger, while the result of the FFRLS method is stable at 51.716 $\mu\Omega$.

Therefore, the tRMSE between the resistance measured by the FFRLS method and the conventional true value is calculated to analyze the accuracy of the methods as the current varies. The tRMSE with different time-varying current modes is shown in table 2. The tRMSE of the average method reaches a maximum of 28.212 $\mu\Omega$, while the error of the proposed method is less than 1.997 $\mu\Omega$. This indicates that the FFRLS method measures the resistance more accurately than the average method as the current varies. Random error evaluation of the new method is carried out and the population standard deviation σ is mainly evaluated with equation (14), which is distributed in ± 1.919 $\mu\Omega$.The measurement error of the FFRLS method with the time-varying current mode is mostly smaller than 6 $\mu\Omega$ at a 99.73% confidence level and meets the monitoring requirements. Furthermore, when welding with time-varying current, the average value of the current differential dI/dt of one cycle no longer decays with time. As a result, the average method cannot eliminate the inductive noise, and the resistance of one cycle $\overline{R_t}$ comes with a large error as the current varies. However, the FFRLS method iterates the current, voltage and current differential dI/dt of each sampling point and then iteratively decouples resistances and inductances effectively regardless of the existence of dI/dt. As long as the variation information of the sampling point

is accurately collected, the accuracy of the results measured by the FFRLS method is ensured. The measurement system mentioned in the article can accurately sample the voltage and current signal as the current varies, thus ensuring the accuracy of the FFRLS method.

Uncoated 0.8 mm DP590 high-strength steel sheets were also used to test the effectiveness and reliability in actual welding with the time-varying current mode, where the electrode force was set to 2.6 kN. Different degrees of current variation dI (1.5 kA, 3 kA and 4.5 kA) and different times of current variation dt (30 ms, 20 ms and 10 ms) shown in figure 10 were also applied in the welding experiments with steel sheets. When the degree of current variation dI is 3 kA and the variation time dt is 30 ms, the two curves are almost the same. It can be seen from figures 12(c)–(f) that the resistance measured by the average method and the FFRLS method is significantly different as the current varies. When the degree of current variation dI increases or the time of current variation dt decreases, the resistance measured by the average method has a larger mutation, which notably reaches 120 $\mu\Omega$ when the dI is 4.5 kA and dt is 10 ms. However, the DR curve measured by the FFRLS method conforms to the law of RSW DR change, and no significant mutation occurs as the current varies. According to the RSW theory, the resistance measured by the FFRLS method is more accurate than the result of the average method as the current varies.

In addition, it is difficult to correctly post-process the mutations caused by the average method. Expulsion may also lead to a mutation in the resistance signal [40, 41]. It is hard to determine whether the mutation is derived from the expulsion or the time-varying current, especially under the time-varying current mode. If the post-processing is performed through a simple linear interpolation, it may result in a misdetection of weld expulsion. In addition, post-processing of the results of

the average method causes lagging in getting results, which cannot realize the real-time monitoring and control of the current welding. Therefore, for a field where high accuracy and fast response are not required, the average method can be used. However, for some high-end scenarios such as welding adaptive control and accurate evaluation of welding quality, the FFRLS method can pave the way for the subsequent studies.

5. Conclusion

In this study, based on the forgetting-factor recursive least squares (FFRLS) algorithm, a novel method was proposed to measure the DR signal in real time during the MFDC RSW process with high measurement accuracy. From the experimental analyses, the following conclusions can be drawn.

(a) The novel method can decouple resistance and inductance correctly with the optimal forgetting factor, and the measurement error of this new method is limited within ± 6 $\mu\Omega$ at a 99.73% confidence level ($\pm 3\sigma$). Compared to traditional DR measurement methods such as the root mean square (RMS) method and average method, the new method can eliminate the interference of inductance and meet the monitoring requirements under different welding modes, including constant and time-varying current modes.

(b) The forgetting factor is proven to be the critical parameter of the novel method. When the forgetting factor decreases, the tracking ability of the system becomes stronger but more sensitive to noise. Thus, to balance the convergence speed and oscillation amplitude in the resistance measurement, the forgetting factor is optimized to 0.98.

(c) The resistance measured by the RMS method contains errors caused by inductive noise, but the average method can measure DR correctly when the current is constant. The intercept of the volt–ampere characteristic curve obtained by the RMS method is very large, while the curve obtained by the average method followed the pure resistance load law and its slope can be considered as the conventional true value.

(d) The comparative study has been conducted with the time-varying current mode, and the results show that the average method cannot eliminate inductance noise as the current varies. The average current differential dI/dt in an inverter cycle no longer decays with the increase of time, so the inductive error cannot be eliminated. The faster the current changed, the larger the error became.

The DR curves can be used to monitor the welding process. The FFRLS method can pave the way for subsequent studies in some high-precision and fast-response fields of application such as weld quality evaluation. In addition, intelligent welding control and other related research can be conducted subsequently. In this study, only uncoated high-strength steel materials were used to analyze the performance of the proposed method, so other emerging steels can be further studied.

ORCID iDs

Ze-Wei Su https://orcid.org/0000-0002-7228-7819
Yu-Jun Xia https://orcid.org/0000-0001-6729-8022
Yong-Bing Li https://orcid.org/0000-0002-4081-3386

References

[1] Ceglarek D, Shi J and Wu S M 1994 A knowledge-based diagnostic approach for the launch of the auto-body *Assembly Process J. Eng. Ind.* **116** 491–9
[2] Zhang Y S, Wang H and Chen G L 2007 Monitoring and intelligent control of electrode wear based on a measured electrode displacement curve in resistance spot welding *Meas. Sci. Technol.* **18** 867
[3] Bhattacharya S and Andrews D R 1974 Research and Development-Significance of dynamic resistance curves in theory and practice of spot welding *Weld. Met. Fabr.* **42** 296–9
[4] Savage W, Nippes E F and Wassel F A 1978 Dynamic contact resistance of series spot welds *Weld. J.* **57** 43s–50s
[5] Cho Y and Rhee S 2000 New technology for measuring dynamic resistance and estimating strength in resistance spot welding *Meas. Sci. Technol.* **11** 1173
[6] Garza F J and Das M 2000 Identification of time-varying resistance during welding *IEEE Instrum. Meas. Technol.* **2000** 1534–9
[7] Garza F J and Das M 2001 On real time monitoring and control of resistance spot welds using dynamic resistance signatures *IEEE Int. Midwest Symp. on Circuits Syst.* **2001** 41–4
[8] Ling S F, Wan L X and Wong Y R 2010 Input electrical impedance as quality monitoring signature for characterizing resistance spot welding *NDT&E Int.* **43** 200–5
[9] Wong Y R and Xin P 2014 A new characterization approach of weld nugget growth by real-time input electrical impedance *Engineering* **06** 516–25
[10] Wang L, Hou Y and Zhang H 2016 A new measurement method for the dynamic resistance signal during the resistance spot welding process *Meas. Sci. Technol.* **27** 095009
[11] Zhang H, Hou Y and Tao Y 2018 Welding quality evaluation for the resistance spot welding using the time-varying inductive reactance signal *Meas. Sci. Technol.* **29** 055601
[12] Johnson K I and Needham J C 1972 New design of resistance spot welding machine for quality-control *Weld. J.* **51** 338–51
[13] Podrzaj P, Polajnar I and Diaci J 2004 Expulsion detection system for resistance spot welding based on a neural network *Meas. Sci. Technol.* **15** 592
[14] Kang Z and Cai L 2014 Study on effect of electrode force on resistance spot welding process *J. Appl. Phys.* **116** 2823–30
[15] Wang X F, Li Y B and Meng G X 2011 Monitoring of resistance spot weld quality using electrode vibration signals *Meas. Sci. Technol.* **22** 045705
[16] Martín Ó, López M and Martín F 2007 Artificial neural networks for quality control by ultrasonic testing in

resistance spot welding *J. Mater. Process. Technol.*
183 226–33

[17] Martín Ó, Tiedra P D and López M 2009 Quality prediction
of resistance spot welding joints of 304 austenitic stainless
steel *Mater. Des.* **30** 68–77

[18] Hua L, Wang B and Wang X 2019 *In situ* ultrasonic detection
of resistance spot welding quality using embedded probe *J.
Mater. Process. Technol.* **267** 205–14

[19] Chang H S, Cho Y J and Choi S G 1989 Proportional-
integral controller for resistance spot welding using nugget
expansion *J. Dyn. Syst. Meas. Control* **111** 332–6

[20] Wang H, Zhang Y and Chen G 2009 Resistance spot
welding processing monitoring based on electrode
displacement curve using moving range chart
Measurement **42** 1032–8

[21] Lovro K, Polajnar I and Diaci J 2011 A method for measuring
displacement and deformation of electrodes during
resistance spot welding *Meas. Sci. Technol.* **22** 067002

[22] Chen J Z and Farson D F 2004 Electrode displacement
measurement dynamics in monitoring of small scale
resistance spot welding *Meas. Sci. Technol.* **15** 2419–25

[23] Chen J Z and Farson D F 2006 Modeling small-scale
resistance spot welding machine dynamics for process
control *Int. J. Adv. Des. Manuf. Technol.* **27** 672–6

[24] Cho Y and Rhee S 2003 Experimental study of nugget
formation in resistance spot welding *Weld. J.* **82** 195s–201s

[25] Ouafi A E, Bélanger R and Méthot J 2011 Artificial neural
network-based resistance spot welding quality assessment
system *Int. J. Metall.* **108** 343–55

[26] Chied C S and Jr E K-A 2002 Investigation of monitoring
systems for resistance spot welding *Weld. J.* **81** 195s–9s

[27] Needham C 1983 Measurement of the resistance at high
alternating current *Weld. Inst.* 1–6

[28] Xia Y J, Zhang Z D and Xia Z X 2015 A precision analogue
integrator system for heavy current measurement in MFDC
resistance spot welding *Meas. Sci. Technol.* **27** 25104–11

[29] Kang Z and Cai L 2011 Improvement in control system for the
medium frequency direct current resistance spot welding
system *Proc. Am. Control Conf.* **2011** 2657–662

[30] Wei L, Cerjanec D and Grzadzinski G A 2015 A comparative
study of single-phase AC and multiphase DC resistance
spot welding *J. Eng. Ind.* **127** 583–9

[31] Klopcic B, Dolinar D and Ctumberger G 2008 Advanced
control of a resistance spot welding system *IEEE Trans.
Power Electron.* **23** 144–52

[32] Ma Y, Wu P and Xuan C 2013 Review on techniques for
on-line monitoring of resistance spot welding process *Adv.
Mater. Sci. Eng.* **2013** 630984

[33] Kang Z and Yao P 2017 Review of application of the electrical
structure in resistance spot welding *IEEE Access* **5** 25741–9

[34] Lee D, Morf M and Friedlander B 1981 Recursive least
squares ladder estimation algorithms *IEEE Trans. Acoust.
Speech Signal Process.* **29** 627–41

[35] Han L, Sheng J and Ding F 2009 Recursive least squares
identification for multirate multi-input single-output
systems *Proc. Am. Control Conf.* **2009** 5604–9

[36] Bobrow J E and Murray W 1993 An algorithm for RLS
identification parameters that vary quickly with time *IEEE
Trans. Autom. Control* **38** 351–4

[37] Vahidi A, Stefanopoulou A G and Peng H 2005 Recursive
least squares with forgetting for online estimation of vehicle
mass and road grade: theory and experiments *Veh. Syst.
Dyn.* **43** 31–55

[38] Paleologu C, Benesty J and Ciochina S 2008 A robust
variable forgetting factor recursive least-squares algorithm
for system identification *IEEE Signal Process. Lett.*
15 597–600

[39] Lu L, Zhao H and Chen B 2016 Improved-variable-forgetting-
factor recursive algorithm based on the logarithmic cost for
Volterra system identification *IEEE Trans. Circuits Syst.*
63 588–92

[40] Xia Y J, Su Z and Li Y 2019 Online quantitative evaluation
of expulsion in resistance spot welding *J. Manuf. Process.*
46 34–43

[41] Xia Y J, Su Z W, Lou M, Li Y B and Carlson B E 2019 Online
precision measurement of weld indentation in resistance
spot welding using servo gun *IEEE Trans. Instrum. Meas.*
2019